

PAPER 31 – DEVELOPMENT OF TWO-LEVEL CONTROL TECHNIQUES FOR LOAD FREQUENCY CONTROL IN ISLANDED TWO-AREA MULTISOURCE MICROGRID

N. Abdulazeez¹, Musa Umar², I. N. Yakubu²

¹Department of Electrical Engineering of Ahmadu Bello University, Zaria – Nigeria

²Department of Electrical and Electronics Engineering Technology, Federal Polytechnic Kaura Namoda
Email: abduazeeznurudeen224@gmail.com

ABSTRACT

Microgrid (MG) development has contributed to widespread connections among distributed generation (DG) units. In this paper, a two-area MG system comprise of different micro sources was developed. The dynamic nature of various renewable energy resources (RESs) wind power fluctuations, and changes in applied load are the significant challenges faced in an islanded microgrid (IMG) frequency control. With respect to this, two-level control technique-based load frequency control (LFC) was developed. The aim is to develop a control scheme that maintains zero steady-state errors for deviation in frequency and inter-area power flow within the acceptable limits in two-area IMG. The developed LFC was implemented using a PI controller at a lower level and a PID controller at a high level. Each controller measures and solve the integral of time multiplied absolute error (ITAE) to compute the optimal gain of the PI controller using the quasi-opposition Jaya algorithm (QOJAYA). At the same time, the PID coordinates the activities of the two-area and provides reference signals to the lower-level controllers. The feasibility of the developed scheme was verified through time-based simulations in MATLAB/Simulink environment. Its performances were compared with the Improved Salp Swarm Algorithm Type II fuzzy PID control scheme using settling time and maximum deviation as performance metrics.

KEYWORDS: Islanded microgrid, Microgrid, Load frequency control, Renewable energy Resources.

1. INTRODUCTION

Power energy is one of the key factors for any nation's growth and future prosperity, therefore, there is need to balance power generation and power demand, keeping in mind economic, technical, and environmental reasons for the choice of means of generation of electrical power. One of the major challenges of energy planners is to decide whether the investment in today's energy infrastructure should be based on emerging technology (RESs) or traditional fossil fuels. Renewable energy resources (RESs) are clean sources of energy that are increasingly displacing “dirty” fossil fuels in the power sector (Bayindir *et al*, 2014). The integration of RESs has considerably increased in recent years largely due to its environmental and economic friendly. This gives the concept of microgrid (MG) wider acceptability (Ravindra *et al*, 2014). It simply comprises distributed generators (DGs), energy storage devices, and load confined within an area with a small geographical spanning (Kortz, 2017). An MG can be operated in two modes: Islanded/off-grid mode and the grid-connected mode. Islanded microgrids (IMGs) power systems (PS) provide access to electricity to the rural and remote areas and isolated islands. IMGs differ from the central power grid, in structure, size, and functionality. IMGs consist of various RESs, like Wind and Photovoltaic (PV) which supply unstable power to MG. High penetration of RESs of inverter-based results in low system inertia. The reduced inertia in the MG lead to an increase in the rate of change of frequency, which may, in turn, lead to instability in the MG. Going by the factors mentioned above, IMG frequency control requires an intelligent and efficient controller (Palizban and Kauhaniemi, 2015; and Li *et al*, 2018).

The frequency of a PS depend on the active power balance. As the frequency is a common factor throughout the system, a change in active power demand at one point is reflected throughout the system by a change in frequency. In the islanded mode of operation, generation (having an intermittent source) and loads (demand-based) are varying continuously, so frequency control plays an important role in system stability (Li *et al*, 2018). Frequency control remains one of the most important issues in the power system. Future power systems need more robust and optimal LFC approaches that can handle new challenges posed by modern PS. By considering the aforementioned factors, IMG frequency control requires an intelligent and efficient controller (Palizban and Kauhaniemi, 2015).

To study the dynamic response of IMG against the change in load or source power various mathematical models of IMG have been reported in the literature. The designed of an optimal quasi-oppositional harmony search algorithm (QOHS) based on a load frequency controller was discussed in (Shankar and Mukherjee, 2016), Kayalvizhi and Kumar, (2017) proposed a new centralized fuzzy adaptive MPC for LFC of an IMG, an intelligent ABC-Based terminal sliding mode controller for load-frequency control of islanded micro-grids was presented in (Bagheri *et al*, 2020), in (Han *et al*, 2015), for load frequency in an autonomous MG, a μ -based robust controller

was proposed. Load frequency control method using PSO-based ANN control was presented in (Safari *et al.* 2018), an improved-salp swarm optimization (I-SSO) for LFC in IMG was discussed in (Prakash *et al.*, 2018). However, the control strategies gave a good dynamic response, but they depend on the designer's experience. The aim of this paper is to develop a two-level supervisory load frequency control scheme for maintaining both frequency and tie-line power to their nominal values under different uncertainties. The two level control (i.e., lower level PI and higher level PID) controller is proposed to create necessary IMG control mechanism. The different gain parameters of proposed controllers are optimized by using Quasi-Oppositional JAYA (QO-JAYA) algorithm and finally to justify the supremacy of proposed two level control scheme its performances were compared with type-II fuzzy controller optimized using ISSO.

2 DESCRIPTION OF THE PROPOSED MODEL

For this study, the structure of IMG considered comprises of RESs like wind and PV source, storage sources like battery and flywheel and auxiliary sources like diesel engine generator (DEG), fuel cell (FC) and a micro-turbine (MT). The output of RESs is uncontrolled since it is weather dependent and highly stochastic in nature so there is a need for such controlled sources. These controlled sources i.e. MT, DEG, FC play an important role to stabilize the system when RESs' power is down to continuously supply the load demand. These controlled sources need some definite time to respond and feed the IMG, hence there is a need for such a source that can support the grid until the controlled sources are on. To fulfill this requirement, the storage system is applied which is charging during the normal case (power supply is equal to or more than demand). As soon as there is more demand than supply then storage sources immediately get activated for a shorter period and provide a huge amount of power to balance the demand and supply. The general schematic of the IMG is shown in Figure 1 which shows that distributed resources are integrated to ac bus through power converters.

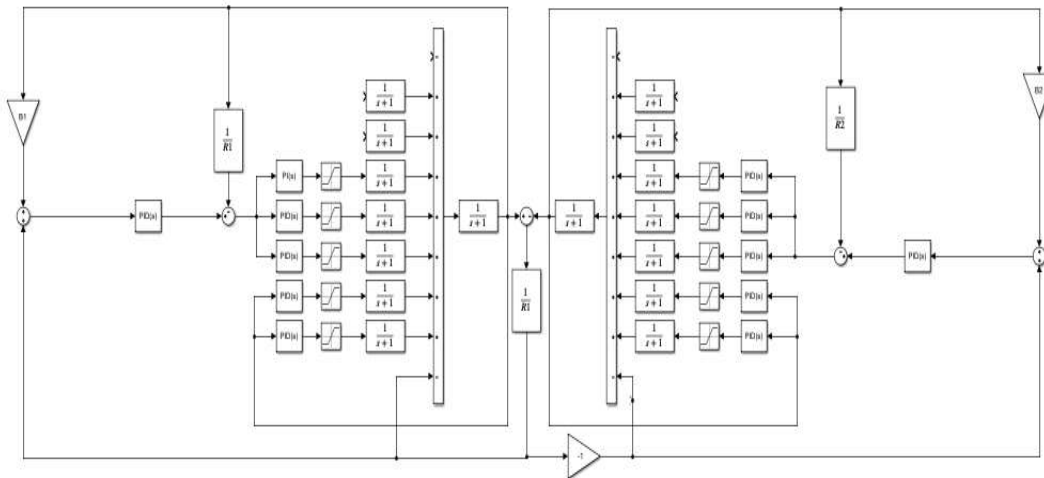


Figure 1: Configuration of a Two-area IMG system

The transfer function expression for the individual system is as shown in equation 1 to 8 (Prakash *et al.*, 2018):

$$\text{Wind turbine generator } (G_{WT}(s)) = \frac{1}{1+ST_{WT}} \quad (1)$$

where T_{WT} is the time constant of the wind turbine

$$\text{Photo Voltaic (PV) } (G_{PV}(s)) = \frac{1}{1+ST_{PV}} \quad (2)$$

where T_{PV} is the time constant of the PV

$$\text{Microturbine } (G_{MT}(s)) = \frac{1}{1+ST_{MT}} \quad (3)$$

where T_{MT} is the time constant of the MT

$$\text{Diesel Generator } (G_{DG}(s)) = \frac{1}{1+ST_{DG}} \quad (4)$$

where T_{DG} is the time constant of the DG

$$\text{Fuel Cell } (G_{FC}(s)) = \frac{1}{1+ST_{FC}} \quad (5)$$

where T_{FC} is the time constant of the FC

$$\text{Flywheel Energy Storage } (G_{FES}(s)) = \frac{1}{1+ST_{FES}} \quad (6)$$

where T_{FES} is the time constant of the FES

$$\text{Battery Energy Storage (G}_{\text{BES}}(s)) = \frac{1}{1+sT_{\text{BES}}} \quad (7)$$

where T_{BES} is the time constant of the BES

The total power generation in each area of the MG system is

$$P_{\text{total}} = P_{\text{DG}} + P_{\text{MT}} + P_{\text{FC}} + P_{\text{WT}} + P_{\text{PV}} \pm P_{\text{BES}} \pm P_{\text{FES}} \quad (8)$$

2.1 Control Topology

In an interconnected (PS) with two or more interconnected control areas (CAs), the generation within each area must be controlled to maintain the load demand with that CA and schedule power interchange with its neighboring CAs. In the LFC problem, each area has its generator or coherent group of generators responsible for a generation. The tie-lines are the utilities through which the contracted and uncontracted (in abnormal conditions) energy exchange between the CAs is provided. In two areas islanding MG, the communication system is required to provide a means to exchange data and monitor various elements for control and protection purposes. In centralized control, a central controller (CC) acts as an interface between all the CAs and the distributed management system. Central control collects data and determines controlling actions for all units. Extensive communication and computation are required in centralized control, this requirement makes the centralized control infeasible (Singh *et al*, 2019). In decentralized control, each unit has a local controller (LC). The units are controlled independently by their LC because decentralized control assumes that the communication between subsystems is negligible. The controller does not rely on control of other controller's action. To achieve reliable and efficient control decentralized approach a strong coupling between the system units is required (Badal *et al*, 2019). As a result of the above situations, a two-level optimal coordination control method for the LFC of the multi-area IMG is preferred over the convention methods for load frequency control due to their computational efficiencies, solution accuracies, and improved reliability. Two-level load frequency control scheme, the lower control level comprised of proportional-integral (PI) to regulate each of the micro-source to control the MG's frequency and inter-MG power exchanges. At the higher control level, a proportional-integral-derivate (PID) will be applied in each MG as a supervisory controller to determine the set-points for the decentralized PI controllers in the lower layer. The control scheme is proposed to have the capability of switching from the two-level supervisory LFC to a decentralized LFC (i.e. comprising of only the local PIs) when the PIDs in the higher level (or communication between them) failed.

3 METHODOLOGY

The objective function for the two-level LFC problem are formulated as follows:

3.1 Formulation of Two-Level based LFC Objective Function

The lower control level comprises of proportional-integral (PI) to regulate each of the micro-source to control the MG's frequency and higher level comprises of PID controller to supervised the control activities of the two CAs. The Integral of Time multiplied Absolute Error (ITAE) criteria is used as the objective function for both the two control level as expressed in equation 9 and 10 respectively.

$$J_{\text{LC}} = \text{ITAE} = \min \int_0^T ACE_i = \int_0^T B \Delta f \quad (9)$$

Where B denotes the biasing factor and Δf is the frequency deviation in p.u.

$$J_{\text{HC}} = \text{ITAE} = \int_0^T ACE_i, \quad \text{for } i=1,2 \quad (10)$$

$$ACE_1 = B \Delta f + \Delta P_{\text{tie}}$$

where ΔP_{tie} change in tie-line power between the ith area and the other area.

While minimizing ITAE the following constraints are need to be maintained

- i. Load-generation balance as equality constraint as expressed in equation (11)

$$\sum P_{G_i} = \sum P_{D_i} + P_i^{\text{tie}}(t) \quad (11)$$

- ii. Frequency band: the frequency is constrained within the certain upper and lower band as;

$$f_i^{\min} \leq f_i \leq f_i^{\max} \quad (12)$$

- iii. Controller gains constraints: the controller proportional, integral, and derivate gains are constrained with some upper and lower limits for practical considerations, as shown in (13-15);

$$K_{pi}^{\min} \leq K_{pi} \leq K_{pi}^{\max} \quad (13)$$

$$K_{li}^{\min} \leq K_{li} \leq K_{li}^{\max} \quad (14)$$

$$K_{Di}^{\min} \leq K_{Di} \leq K_{Di}^{\max} \quad (15)$$

3.2 Quasi-Oppositional Jaya (QO-JAYA) Algorithm

QO-Jaya algorithm is developed for solving multi-objective optimization problems (Rao et al. 2017). In the QO-Jaya algorithm, the task of finding the best and worst solutions is accomplished by comparing the rank assigned to the solutions based on the non-dominance concept and the crowding distance value.

In the beginning, an initial population is randomly generated with a P number of solutions. Then a quasi-opposite population is generated which is combined with the initial population. This combined population is then sorted and ranked based on the non-dominance concept and the crowding distance value is computed for each solution. The quasi-opposite population is generated using equation (16).

$$X_{ij}^q = rand(a, b) \quad (16)$$

$$a = \frac{L+U}{2} \quad (17)$$

$$b = L + U - X_{ij} \quad (18)$$

Where L and U are the lower and upper bound of the variable; X_{ij}^q is the quasi-opposite value of X_{ij} .

Then P best solutions are selected from the combined population-based on rank and crowding distance. Further, the solutions are modified according to equation (19).

$$A(i + 1, j, k) = A(i, j, k) + r(i, j, 1)(A(i, j, b) - |A(i, j, k)|) - r(1, j, 2)(A(i, j, w) - |A(i, j, k)|) \quad (19)$$

Here b and w represent the index of the best and worst solutions among the current population. i, j, k are the index of iteration, variable, and candidate solution.

$A(i, j, k)$ means the jth variable of kth candidate solution in an ith iteration. $r(i, j, 1)$ and $r(i, j, 2)$ are numbers generated randomly in the range of [0, 1]. The random numbers $r(i, j, 1)$ and $r(i, j, 2)$ act as scaling factors and ensure good diversification.

For this purpose, the best and worst solutions are to be identified. The solution with the highest rank (rank = 1) is selected as the best solution. The solution with the lowest rank is selected as the worst solution. The number of function evaluations required by the MOQO-Jaya algorithm = population size * no. of generations for a single simulation run.

i. Non-dominated Sorting of the Population

In this approach the population is sorted into several ranks (fronts) based on the dominance concept as follows: a solution x_i is said to dominate other solution x_j if and only if solution x_i is no worse than solution x_j concerning all the objectives and the solution x_i is strictly better than solution x_j in at least one objective. If any of the two conditions are violated, then solution x_i does not dominate solution x_j . Among a set of solutions P, the non-dominated solutions are those that are not dominated by any solution in the set P.

ii. Constraint-Dominance Concept

A solution i is said to constrained-dominate a solution j, if any of the following conditions is true. Solution i is feasible and solution j is not. Solutions i and j are both infeasible, but solution i has a smaller overall constraint violation. Solutions i and j are feasible and solution i dominates Solution j.

iii. Crowding Distance Computation

The crowding distance is assigned to each solution in the population to estimate the density of solutions surrounding a particular solution i. Thus, the average distance of two solutions on either side of solution i is measured along each of the M objectives. This quantity is called the crowding distance (CD_i).

$$CD_j = CD_j + \frac{f_m^{j+1} - f_m^{j-1}}{f_m^{max} - f_m^{min}} \quad (20)$$

where j is a solution in the sorted list, f_m is the objective function value of mth objective, f_m^{max} and f_m^{min} are the population-maximum and population-minimum values of the mth objective function.

i. Crowding-Comparison Operator

Crowding-comparison operator is used to identifying the superior solution among two solutions under comparison, based on the two important attributes possessed by every individual i in the population i.e. non-domination rank (Rank_i) and crowding distance (CD_j).

3.3 Algorithm for Optimal Tuning of PI and PID Controller Parameter Using QO-Jaya Algorithm

- i. Read input data i.e., frequency, active power generation limits of all controllable DGs, and constraints.
- ii. Read algorithm parameters i.e. population size, maximum number of iterations, and declaration of both upper bound and lower bound of variables.
- iii. Generate quasi-opposite population using equation (16)
- iv. Select good (P) solutions from initial population and quasi-opposite
- v. Perform greedy selection to identify best and worst solutions in the selected population using equation (20) and compute new solution using equation (19).
- vi. If the new position is better than old.
- vii. Evaluate the objective function for the two control level
- viii. Repeat steps (iv) to (vii) until a convergence criterion is met.

ix. Stop and print the result

4. RESULTS AND DISCUSSION

This section presents the two different analysis to validate the effectiveness of the proposed two-level control scheme upon the type II fuzzy controller based ISSO. The time-domain simulation results are presented to show the superiority of the developed scheme for the IMG system stability subjected to perturbation in ΔPL and ΔPW . The study of frequency deviation by changing the load and wind power has been recorded.

Case 1: Time-domain simulation results for frequency deviation against load power deviation ΔPL by type II fuzzy controller based ISSO and two-level control scheme

In this case, the solar irradiation and wind speed are considered constant and a random pattern load as shown in Figure 2a is effected in the IMG at time $t=0$. In regard to this disturbance, the deviated responses of frequency and tie-line power resulted due to the two-level controller is depicted in this section. The deviation in frequency of area1 and area2 due to QO-Jaya optimized controllers are shown in Figure 2 (b-c) respectively. The tie-line power deviation is given in Figure 2 (d).

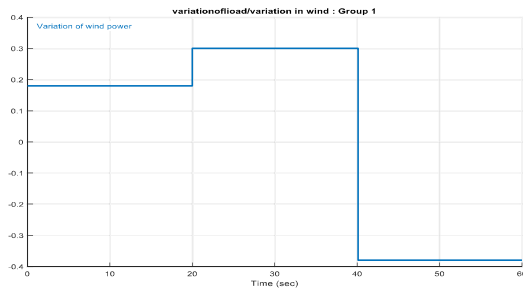


Figure 2a: Variation of load (ΔPL)

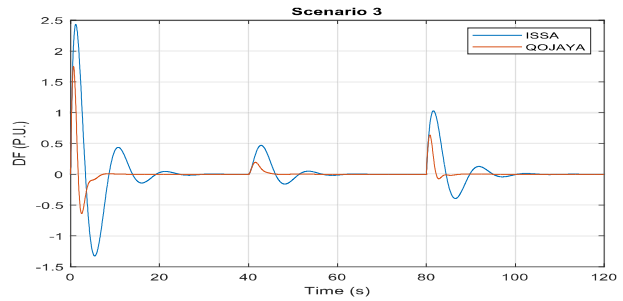


Figure 2b: Variation of area1 frequency due to ΔPL

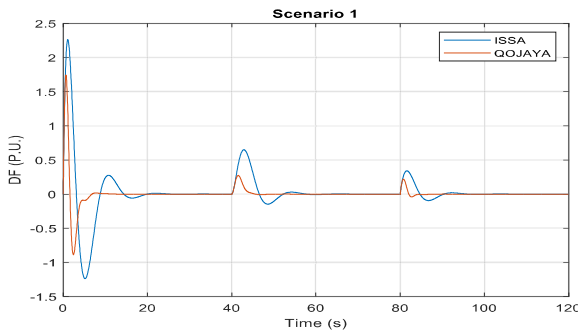


Figure 2c: Variation of area2 frequency due to ΔPL

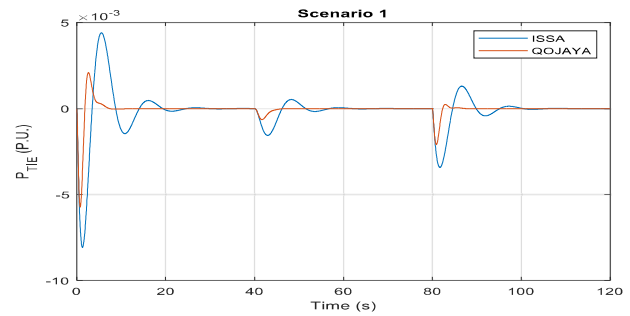


Figure 2d: Variation of tie-line power due to ΔPL

Case 2 Wind Power Fluctuation (ΔP_{Wind})

In this case, the wind turbine is considered as white noise since the environmental fluctuations are continuous and unstable. Figure 3a shows the wind power perturbation and Figure 3(b-c) represents the MG output frequency response by comparing the proposed controllers. The tie-line power deviation is given in Figure 3 (d).

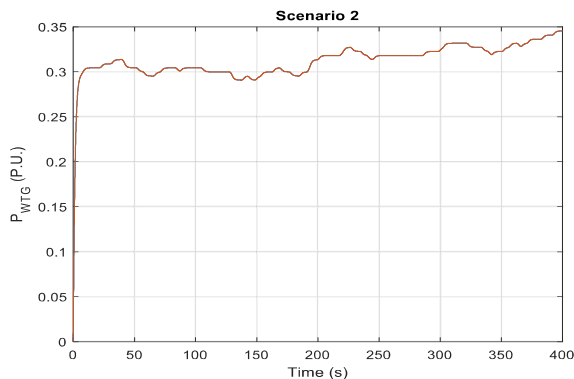


Figure 3a: Variation of wind power (ΔPW)

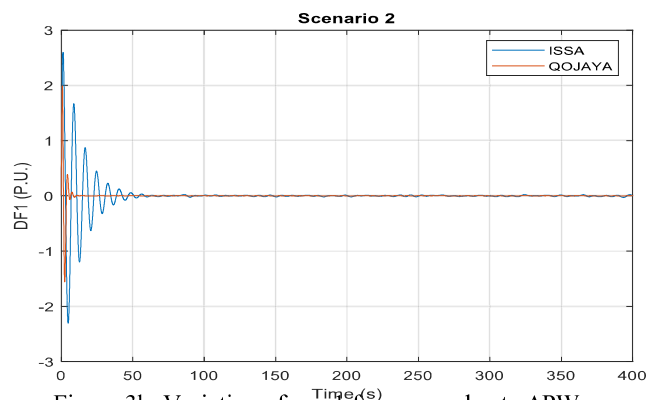


Figure 3b: Variation of area1 frequency due to ΔPW

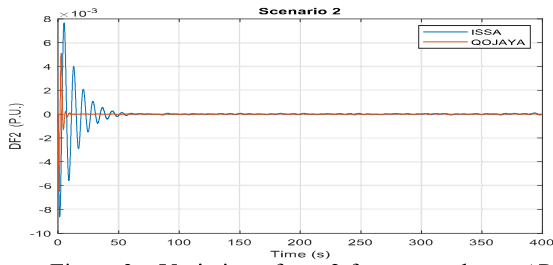


Figure 3c: Variation of area2 frequency due to ΔPW

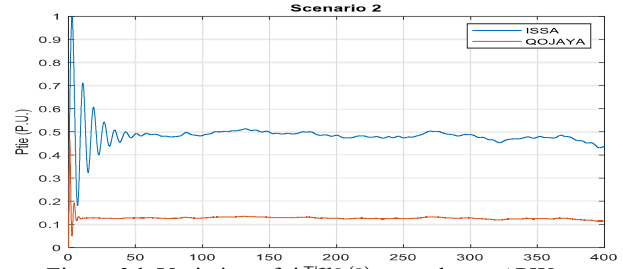


Figure 3d: Variation of tie-line power due to ΔPW

The critical analysis on dynamic responses and Table.1 reveals that, the proposed control scheme outperformed the ISSA tuned type-II fuzzy PID controller.

Table 1: Summary of two area IMG Response Following RLP with ISSA-Type II Fuzzy PID and Proposed Controller

States	Controller	Performance			
		Settling time (sec)	Improvement	Maximum deviation	Improvement
f_1 (Hz)	Proposed Control	4.79	29.556%	-0.0007	30%
	ISSA	6.80		-0.001	
f_2 (Hz)	Proposed Control	4.63802	25.161%	0.00	0%
	ISSA	6.20		0.00	
DP_{tie}	Proposed Control	5.18	19.32%	0.00018	21.74%
	ISSA	6.42		0.00023	
ITAE	Proposed Control	8.2523	6.367%		
	ISSA	8.8312			

The dynamic responses has been depicted through different conditions reveal that proposed control scheme exhibits more effectiveness over ISSA optimized type-II fuzzy PID controller. Overall critical discussions on this section reveal that proposed control scheme exhibits superior performance in regard to LFC study of an islanded multi-area interconnected MG system.

5. CONCLUSION

In this work, a two level control scheme is proposed for the comprehensive LFC analysis of a multi-area multisource interconnected islanded microgrid system. The developed control schemes are meant to enable both centralization and decentralization of power system. The proposed controller simulation outcomes are compared with the Type II fuzzy PID control scheme under different scenarios. From the simulation outcomes of all scenarios, the proposed controller exhibits a better dynamic performance in terms of fast settling time, overshoot reduction and less frequency deviation error over Type II fuzzy PID controller.

REFERENCES

- Annamraju A. and Nandiraju S. (2018): Robust Frequency Control in an Autonomous Microgrid: A Two-Stage Adaptive Fuzzy Approach, Electric Power Components and Systems, DOI: 10.1080/15325008.2018.1432723.
- Bagheri, A., Jabbari, A., and Mobayen, S. (2020). An Intelligent ABC-Based Terminal Sliding Mode Controller for Load-Frequency Control of Islanded Micro-Grids. Sustainable Cities and Society, 102544. doi:10.1016/j.scs.2020.102544.
- Bayindir, R., Hossain, E., Kabalci, E., and Perez, R. (2014). "A Comprehensive Study on Microgrid Technology. International Journal of Renewable Energy Research, 4(4),1094-1107.
- Kayalvizhi S. and Vinod Kumar D. M., (2017) "Load Frequency Control of an Isolated Micro Grid Using Fuzzy Adaptive Model Predictive Control," in IEEE Access, 5,. 16241-16251, 2017, doi: 10.1109/ACCESS.2017.2735545.
- Kortz D. (2017) Microgrids: reliable power is a small package. Barkely Lab Science Beat., <http://www.lbl.gov/science-articles/Archive/EETD-microgrids.html>.
- Li J., Liu Y., Wu L., (2018), Optimal Operation for Community-Based Multi-Party Microgrid in Grid-Connected and Islanded Modes, IEEE Transactions on Smart Grid. 9(2) (2018)756-765.

- Mishra, D., Nayak, P. C., and Prusty, R. C. (2020). PSO optimized PIDF controller for Load-frequency control of A.C Multi-Islanded-Micro grid system. 2020 International Conference on Renewable Energy Integration into Smart Grids: A Multidisciplinary Approach to Technology Modelling and Simulation (ICREISG). doi:10.1109/icreisg49226.2020.9174552.
- Palizban O., Kauhaniemi K., (2015) Hierarchical control structure in microgrids with distributed generation: Island and grid-connected mode, *Renewable and Sustainable Energy Reviews*. 44 (2015) 797-813.
- Prakash C. S., Sonalika M., Ramesh C. P., Sidhartha P. (2018) Improved -salp swarm optimized type-II fuzzy controller in load frequency control of multi area islanded AC microgrid, *Sustainable Energy, Grids and Networks* (2018), <https://doi.org/10.1016/j.segan.2018.10.003>
- Rao, R. V., and Rai, D. P. (2017a). Optimization of welding processes using quasi oppositional based Jaya algorithm. *Journal of Experimental and Theoretical Artificial Intelligence*, 29(5), 1099–1117.
- Ravindra K. Kannan B. Ramappa. N (2014) “Microgrid a Value-Based Paradigin, the need for the redefinition of microgrids, *IEEE Elect Mag* 2(1); 20-29.
- Sanjari M. J. and Gharehpetian G. B., (2013) Small Signal Stability Based Fuzzy Potential Function Proposal for Secondary Frequency and Voltage Control of Islanded Microgrid, *Electric Power Components and Systems*, 41:5, 485-499.
- Shankar, G., and Mukherjee, V. (2016). Load frequency control of an autonomous hybrid power system by quasi-oppositional harmony search algorithm. *International Journal of Electrical Power and Energy Systems*, 78, 715–734.

APPENDICES

Di = damping coefficient ith area = 0,012 (pu/Hz); Mi = Inertia constant of ith area = 0.2 (pu/s); i= 1,2; TFC = Fuel Cell time constant = 4s; TBES = Battery energy time constant = 0.1s; TFES = Flywheel energy storage time constant =0.1s; TDEG = Diesel engine generator time constant = 2s; TMT = Microturbine time constant = 2s; TWTG = Wind turbine generator time constant = 1.5s; TPV = Photo Voltaic cell time constant = 1.8s. B = Frequency biasing factor = 0.425 pu MW /Hz. ; R = Regulation =0.05 Hz/Mw; T12 = Time coefficient=1.6 s.